DETC2018-86288

SOCIAL FORCE CONTROL FOR HUMAN-LIKE AUTONOMOUS DRIVING

DoHyun Daniel Yoon
Clemson University International Center of
Automotive Research
Greenville, SC, USA

Beshah Ayalew
Clemson University International Center of
Automotive Research
Greenville, SC, USA

ABSTRACT

An autonomous driving control system that incorporates notions from human-like social driving could facilitate an efficient integration of hybrid traffic where fully autonomous vehicles (AVs) and human operated vehicles (HOVs) are expected to coexist. This paper aims to develop such an autonomous vehicle control model using the social-force concepts, which was originally formulated for modeling the motion of pedestrians in crowds. In this paper, the social force concept is adapted to vehicular traffic where constituent navigation forces are defined as a target force, object forces, and lane forces. Then, nonlinear model predictive control (NMPC) scheme is formulated to mimic the predictive planning behavior of social human drivers where they are considered to optimize the total social force they perceive. The performance of the proposed social force-based autonomous driving control scheme is demonstrated via simulations of an ego-vehicle in multi-lane road scenarios. From adaptive cruise control (ACC) to smooth lane-changing behaviors, the proposed model provided a flexible yet efficient driving control enabling a safe navigation in various situations while maintaining reasonable vehicle dynamics.

INTRODUCTION

The development of advanced human driver models has been at the center of automotive research for several decades. From maneuver planning, lane change, to collision avoidance, numerous variants of driver models have been developed for traffic simulation studies as well as for refining advanced driver assistance systems (ADAS) [1][2][3]. One critical issue that many studies emphasize is the importance of developing human-like driver models. The introduction of fully autonomous vehicles in the near future will create a new hybrid traffic where human operated vehicles (HOVs) and fully autonomous vehicles (AVs) coexist. In such a traffic environment, the interaction between the two groups is inevitable and understanding the human-like psychological decision-making and planning processes becomes a crucial factor. A human-like social driver model will surely benefit in the development of AVs as well as the understanding of interactions of human drivers and AVs in mixed/hybrid traffic [4][5][6].

An early version of the social force model (SFM) was first proposed in 1998 by Helbing [7] to model pedestrian movements. Social forces represent a measure for the internal motivations of the individuals to perform desired actions. While it is not a physical measure of any direct force, it can be interpreted as a psychological pressure that is indirectly exerted from the environment. Helbing [7] divided the social force into three different types for pedestrian applications: destination force, repulsive force, and attractive force. Destination force describes the willingness to reach the destination, which is the main drive force to move the subject forward. Repulsive force describes the subject's intention to avoid obstacles while attractive force represents the opposite behavior.

Similar social forces can be conceived to be at play when humans operate/drive vehicles in traffic. In particular, one can identify target force/attractor associated with reaching a destination, object forces/repulsors for collision-avoidance, and lane forces for road lane keeping. In this paper, we detail how these constituent forces may be modeled and used for vehicle control/driver modeling.

A number of researchers have already shown promising results of implementing the SFM in vehicular traffic. Li [8] analyzed the collision risk of bicycle-car in a shared space by using SFM to model the interactions among the subjects in the traffic. Qu [9] also studied a mixed flow of electric bike-car and established a microscopic model that simulates the flow. Using the same model, Guo [10] demonstrated a lane-changing behavior of a vehicle in a car-only traffic but without considering vehicle dynamics. All of the studies above did not adopt any control strategy to optimize the input of the ego vehicle nor significantly modify the pedestrian SFM to enhance its

performance. Weinan [11] was the first to use a vehicle dynamics model and to implement PID control transforming the social forces into control inputs. Therein, the steering angle was computed by a simple PID controller, the acceleration of the vehicle was managed by a rule-based control. Unlike Helbing [7] and most of the studies mentioned above which only use SFM to model the equation of motion for multiple agents (pedestrians or vehicles), this work performs an optimization of the total social force to guide the vehicle.

We propose a human-like autonomous driver model using SFM in a nonlinear model predictive control (NMPC) framework. The NMPC framework is a natural choice as the predictive constrained optimization seems to parallel or at least model the navigation decisions made by human drivers. Based on the data received through sensory perception, human drivers endeavor to predict and analyze the behavior of other vehicles before executing the next move. The generic framework of NMPC bears a resemblance to such a process very well. This has been explored in previous studies, [12] and [13], starting with Prokop [14]. In this paper, we detail the NMPC formulation where we consider the driver to optimize the total social force experienced in the presence of obstacles, lanes and a description of a target.

In mathematical terms, this formulation differs from other NMPC formulations proposed for autonomous vehicle guidance [15], where cost functions involved path and speed tracking errors while obstacles and lanes are expressed as constraints, including in probabilistic terms [16]. Therein, finite state machines (FSMs) or rules are often listed to dictate lane change and other pre-defined discrete driving states [15][17]. These are executed outside optimization or result in mixed integer programs (as in choosing between lanes), which in turn require a relaxation that increases the dimensionality of the optimization problem to be solved at every update [18] (e.g. by a number of lane selection variables). The formulation presented here, however, does not require such rule-based assigners for treatment of lanes or objects. The overall concept of the presented approach rather resembles potential field methods (PFM) [19][20]. By minimizing the social force potentials along the path of travel, it provides an alternative method for formulating autonomous driving without additional rules or such accommodations [17].

MODELING DETAILS

In this section, the system models are described in detail. The overview of the proposed control scheme is presented in FIGURE 1. Object vehicle locations and speeds are detected through environmental perception and transmitted to the NMPC. Inside of the controller, the SFM as well as the vehicle dynamics model are used to compute an optimization of the inputs which are then passed to the ego vehicle. By continuously evaluating the current state of the ego vehicle as well as the environment, NMPC provides a human-like autonomous driver behavior.
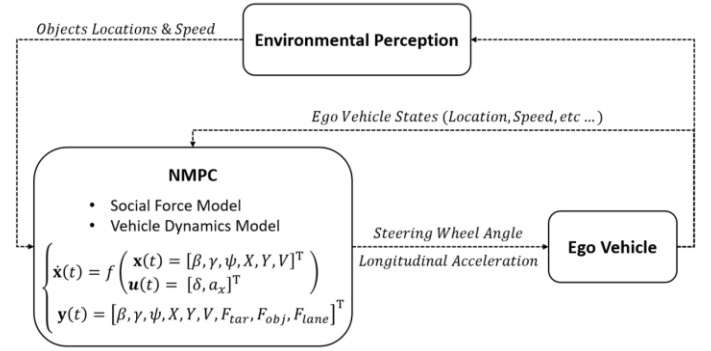

FIGURE 1. OVERVIEW OF THE PROPOSED FRAMEWORK

I. Social Force Model
1) Target Force

The purpose of the target force is to encourage the vehicle to reach the target as soon as possible. Helbing [7] defines the target force as a function of the difference between the current and the desired velocity vector. For vehicular applications, X and Y coordinates do not share the same order of magnitude due to the dimensions of the roads where the longitudinal axis is significantly longer than the lateral axis. This means that the influence of the change in Y coordinates is minimal especially when the target is distant from the current position. Also, this formation allows the target force to be negative which can be undesirably compensated by other forces. To accomplish the main purpose of the target force F_{tar}, the formulation is modified as a scalar quadratic function:

$$F_{tar} = \left(V_{ego} - V_{max}\right)^2 \qquad (1)$$

where V_{ego} is the current ego vehicle speed and V_{max} is the maximum allowable speed on the road. Minimizing this target force encourages the vehicle to continuously attempt to maintain the maximum velocity thereby ensuring the vehicle to travel as far as possible.
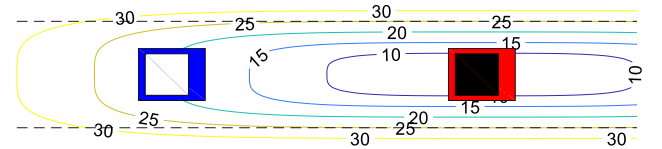

FIGURE 2. AN EXAMPLE OF HYPERELLIPSE OBJECT FORCE EQUIPOTENTIAL LINES (BLUE: EGO VEHICLE, RED: OBJECT VEHICLE)

2) Object Force

Object force is the most important social force that manages collision-avoidance. While driving, drivers keep a certain distance from another vehicle or other objects that may be static or moving on the road. The closer to other objects, the safety concern tends to increase. Such forces can be represented as repulsive forces acting on the main vehicle:

$$F_{obj} = -\nabla_{\vec{r}_o} M_{obj}(S_s, D_{BD}) \qquad (2)$$

where $\vec{r}_o$ is the relative position vector of the object, and $\nabla_{\vec{r}_o}$ represents the divergence of vector $\vec{r}_o$. $M_{obj}(S_s, D_{BD})$ represents a monotonic decreasing function:

$$M_{obj}(S_s, D_{BD}) = K_1 \left(\frac{1}{S_s - D_{BD}} - \frac{1}{D_{LAH} - D_{BD}} \right) \qquad (3)$$

where D_{BD} $(\approx V_{ego} \cdot t_b)$ is the braking distance with the approximate braking time t_b $(= 2 \ or \ 3s)$, D_{LAH} $(= 200\text{m})$ is the look-ahead visual distance of the vehicle, K_1 is a scaling factor, and S_s represents the major axis of a hyperellipse, forming layers of equipotential lines as:

$$S_s = \sqrt{\frac{1}{K_2^n} (X_j - X_{ego})^n + (Y_j - Y_{ego})^n} \qquad (4)$$

where (X_{ego}, Y_{ego}) is the position coordinates of the ego vehicle, (X_j, Y_j) is the position coordinates of the object j $(j = 1, \ldots, N_{obj})$ where N_{obj} is the number of objects in vision, n is the order of the hyperellipse, and K_2 is the ratio of the major to the minor axis of the hyperellipse. The ratio should be determined such that the major longitudinal axis is significantly longer than the minor lateral axis, close to the ratio of the look-ahead distance to the individual lane width. The layers of equipotential lines are shown in FIGURE 2. The formulation of the function M_{obj} allows the object force rise to infinity as the distance between the vehicle and the object nears the braking distance, $\lim_{S_s \to D_{BD}} M_{obj}(S_s, D_{BD}) = \infty$, ensuring that no other social force component (target, lane, etc) can dominate the object force.

3) Lane Force

In addition to the object force, there should be another set of repulsive forces from the road lanes to keep the vehicle at the center of the current lane. Our lane force formulation consists of two different parts. Assuming that the lane center reference is available, the first part of the lane force can be formulated as:

$$F_{cen} = \nabla_{\vec{r}_l} (Y_{ego} - L_{ref,i})^2 \qquad (5)$$

where $L_{ref,i}$ is the lane center reference of lane i, and $\vec{r}_l$ is the relative position vector between the lane center reference to the ego-vehicle. Lane identification is done by using a set of sigmoid functions defined by upper and lower bounds:

$$Sig_i(Y) = \frac{1}{1 + e^{-k(Y - L_{lower_i})}} - \frac{1}{1 + e^{-k(Y - L_{upper_i})}} \qquad (6)$$

where Y is the lateral coordinate of the vehicle, L_{upper_i} and L_{lower_i} are the bounds of each lane i $(1 \ldots N_{lane})$, and k is a constant that governs the slope of the sigmoid function.

The second part of the lane force is to track the yaw angle error in a reference to the curvature of the road. This is defined as:

$$F_{agl} = (\psi_{ego} - \theta_l)^2 \qquad (7)$$

where ψ_{ego} is the yaw angle of the ego vehicle and θ_l is the angle representing the curvature of the road. This will ensure that vehicle heading angle is aligned with the curvature of the road. This portion of the lane force is important especially for stabilizing lateral motion of the vehicle during lane-change. With weighting factors W_{cen} and W_{agl} for each part of the lane force, the total lane force is defined as:

$$F_{lane} = W_{cen} F_{cen} + W_{agl} F_{agl} \qquad (8)$$

II. Vehicle Dynamics Model

For the purposes of demonstrating the framework, we use the bicycle model for a front steered vehicle [21], although higher-order vehicle models can also be used:

$$mV(\dot{\beta} + r) + ma_x \beta = -(C_1 + C_2)\beta - \frac{1}{V}(aC_1 - bC_2)r + C_1 \delta$$

$$J_z \dot{r} = (-aC_1 + bC_2)\beta + \frac{1}{V}(-a^2 C_1 - b^2 C_2)r + aC_1 \delta \qquad (9)$$

$$\dot{V} = a_x$$

where m is the mass of the vehicle, V is the speed, C_1 and C_2 are the cornering stiffness of the front and the rear tires, a and b are the distance between the center of gravity to the front and the rear axle, and J_z is the polar moment of inertia of the vehicle around its center of gravity. β is the body side slip angle, r is the yaw rate of the vehicle, δ is the steering angle, and a_x is the longitudinal acceleration. Powertrain/braking system dynamics, external forces and external moments (due to grade, banking, wind, etc) are ignored here for the sake of simplicity. FIGURE 3 shows the overview of the vehicle bicycle model.
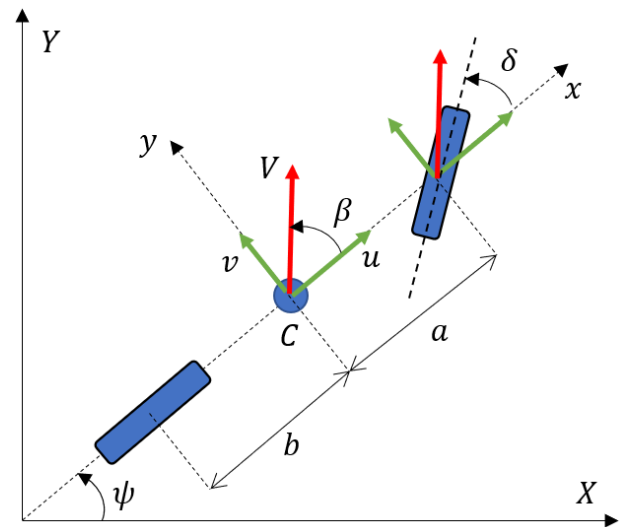

FIGURE 3. VEHICLE BICYCLE MODEL

The trajectory of the vehicle can be computed as:

$$X = \int_0^t V[cos\beta cos\psi - sin\beta sin\psi]\, dt$$
$$Y = \int_0^t V[cos\beta sin\psi - sin\beta cos\psi]\, dt \tag{10}$$

where the yaw angle, ψ is obtained from the yaw rate as:

$$\psi(t) = \int_0^{t_f} r(t)\, dt \tag{11}$$

III. State Space Model of the Overall System

The state space model of the overall system can be assembled considering the body slip angle, the yaw rate, the yaw angle, the X and Y coordinates, and the vehicle speed as the states of the system; the road steering angle and the vehicle longitudinal acceleration as the inputs; and all of the state variables and social forces as outputs.

$$\begin{bmatrix} \dot\beta \\ \dot\gamma \\ \dot\psi \\ \dot X \\ \dot Y \\ \dot V \end{bmatrix} = \begin{bmatrix} -(\frac{C_1+C_2}{mV}+\frac{a_x}{V})\beta - \left(1+\frac{1}{mV^2}(aC_1-bC_2)\right)\gamma + \frac{C_1}{mV}\delta \\ -\frac{(aC_1-bC_2)}{J_z}\beta - \frac{1}{J_zV}(a^2C_1+b^2C_2)\gamma + \frac{aC_1}{J_z}\delta \\ \gamma \\ V(cos\beta cos\psi - sin\beta sin\psi) \\ V(cos\beta sin\psi - sin\beta cos\psi) \\ a_x \end{bmatrix} \tag{12}$$

Then, the model of the system can be written compactly as:

$$\begin{cases} \dot{\mathbf{x}}(t) = f\big(\mathbf{x}(t), \mathbf{u}(t)\big) \\ \mathbf{y}(t) = [\beta, \gamma, \psi, X, Y, V, F_{tar}, F_{obj}, F_{lane}]^\mathrm{T} \end{cases} \tag{13}$$

where the states $\mathbf{x}(t) = [\beta, \gamma, \psi, X, Y, V]^\mathrm{T}$, the inputs $\mathbf{u}(t) = [\delta, a_x]^\mathrm{T}$, and f is a vector function representing mainly the right hand side of (12). Due to the state-dependent vehicle dynamics, the overall system is nonlinear.

NONLINEAR MODEL PREDICTIVE CONTROL

In this section, a nonlinear model predictive control (NMPC) algorithm [22] is formulated for the proposed social force control scheme. NMPC, which is also called receding horizon control, consists of iterative finite-horizon nonlinear optimization. In general terms, NMPC explores the future state trajectory based on the current state with the dynamics model to find a sequence of inputs that minimizes the defined cost for a given prediction horizon. Then, at each update, the first part of the input sequence is implemented, new measurements are collected/states are updated, and the process repeats from the new current state shifting the prediction horizon forward. NMPC is attractive because it can readily handle input and state constraints within the optimization.

As mentioned in the introduction, the receding horizon constrained optimization of NMPC has a resemblance to the human-driver decision making process. In the present context, the objective of NMPC is cast as one of optimizing the total social force, which is a measure of internal motivation or psychological pressure that drivers, or their autonomous counterparts, wish to minimize while allowing the vehicle to maneuver safely and as fast as possible. Given the above models of the social force components, the total social force is the cost function to be minimized:

$$F_{tot} = W_{tar}F_{tar} + W_{obj}F_{obj} + W_{lane}F_{lane} \tag{14}$$

where the cost function $F_{tot}(t)$ is the weighted sum of all social forces with weighting factors W_{tar}, W_{obj}, and W_{lane}. Each social force component needs to be weighted to balance the possible ranges of all three social forces since each force has different orders of magnitude. The weight of the object force must be carefully adjusted to ensure reasonable, safe collision-avoidance behavior. However, only minimizing the social force does not guarantee feasible vehicle control without taking the control inputs into consideration. Therefore, the inputs of the system are added to the cost function by modifying the cost function as follows:

$$L(t) = W_{tar}F_{tar} + W_{obj}F_{obj} + W_{lane}F_{lan} \\ + W_\delta\delta^2 + W_a a_x^2 \tag{15}$$

where W_δ and W_a are the weighting factors for the road wheel steering angle and the vehicle longitudinal acceleration. In order to enforce the vehicle velocity to stay in a reasonable range, it is bounded to a positive range from 0 to V_{max} where V_{max} is defined by the road speed limit. The control inputs will be constrained (by simple bounds) to the available actuation limits. The Y coordinate of the vehicle is constrained so that the vehicle does not cross the edges of the road. As mentioned above, each road lane is not constrained here, and lane-keeping or change is done as a function of the dominance of the lane force in the total social force. This is a distinction vs. other formulations which list hard constraints for lane limits, thereby requiring rule-based schemes for switching lane references outside of the NMPC optimization [15][23].

The optimization problem at each NMPC update is formulated as:

minimize: $\quad J(t) = L_F(t+T_h) + \int_t^{t+T_h} L(\tau)d\tau$

subject to: $\quad \begin{cases} \dot{\mathbf{x}}(t) = f\big(\mathbf{x}(t), \mathbf{u}(t)\big) \\ \alpha_{x,min} \le \alpha_x \le \alpha_{x,max} \\ \delta_{min} \le \delta \le \delta_{max} \\ L_{min} \le Y \le L_{max} \\ 0 \le V \le V_{max} \end{cases} \tag{16}$

where t is the time at every NMPC update and T_h is the prediction horizon, α_{max} and α_{min} are the maximum and the minimum allowable acceleration of the vehicle, δ_{max} and δ_{min} are the maximum and the minimum allowable road steering angle of the

vehicle, L_{max} and L_{min} are the left and the right edges of the road (not individual lanes), and V_{max} is the maximum allowable speed of the road. To mimic the concept of endpoint constraints that ensure with stability of the NMPC scheme, a large weight is posed on the object force in the terminal cost to achieve a desirable convergence.

TABLE 1. INITIAL CONDITION OF THE FIRST SCENARIO

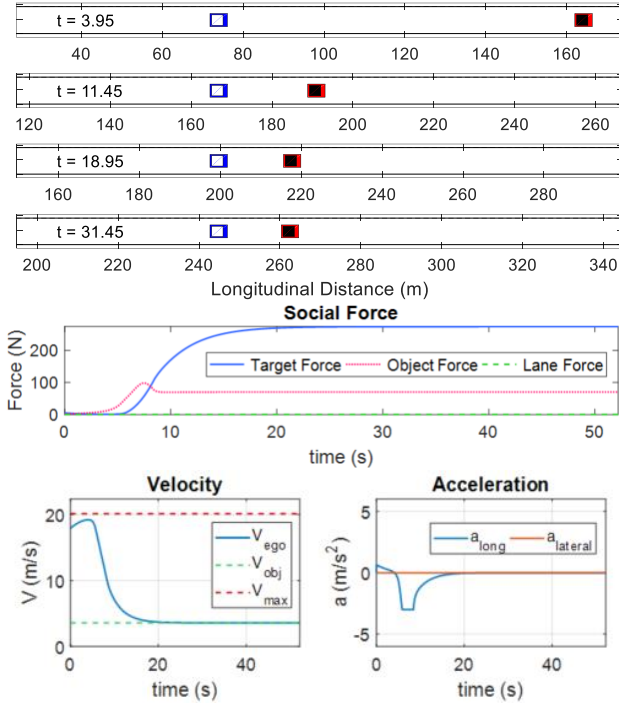| Vehicle	X (m)	Lane Number	V (m/s)
Ego	0	1	17.89
Object 1	150	1	3.58

FIGURE 4. RESULTS OF THE FIRST SCENARIO (BLUE: EGO VEHICLE, RED: OBJECT VEHICLE)

RESULTS AND DISCUSSION

To illustrate the performance of the proposed social driver model that may be used for autonomous driving in hybrid traffic, we simulated several scenarios. The basic parameters of the ego-vehicle model are listed in TABLE 4 in the Appendix. Other object vehicles/traffic participants are modeled to travel at constant velocity. For the purposes of the illustrations, the positions and velocities of the object vehicles are assumed available by measurement, and measurement uncertainties are not considered.

Simulations are done for single-lane and multi-lane roads with different initial conditions. The lane identification is numbered from the right to the left as [Lane 1, Lane 2, ..., Lane 4] for 4-lane roads. For each scenario, weighted social forces, lateral trajectory, velocity, acceleration, yaw rate, and road

steering wheel angle history are plotted along with a few snapshots of the traffic on the road.

TABLE 2. INITIAL CONDITION OF THE SECOND SCENARIO

Vehicle	X (m)	Lane Number	V (m/s)
Ego	0	3	17.89
Object 1	220	3	2.24
Object 2	200	4	3.58

FIGURE 5. RESULTS OF THE SECOND SCENARIO (BLUE: EGO VEHICLE, RED: OBJECT VEHICLES)

Copyright © 2018 by ASME

The first scenario represents a case when there is a slow vehicle in a single-lane road. The initial conditions are shown in TABLE 1. A few snapshots along with the vehicle dynamics plots are presented in FIGURE 4. The lateral trajectory, yaw rate, and steering input plots are omitted since there were no dynamics observed. The initial velocities are set as 17.9 m/s (40 mph) and 3.58 m/s (8 mph) for the ego and the object vehicle, respectively. As the NMPC attempts to minimize the cost function (15) by optimizing the inputs, the ego vehicle accelerates to reach the speed limit of the road (20.1 m/s or 45 mph) since the target force is the dominant force due to the initial conditions. The object force starts to increase as the ego vehicle approaches the object vehicle. As the inter-vehicle distance nears the braking distance defined by the object force in (3), the object force becomes the dominant cost in (15). In spite of the increase in the target force, the ego vehicle decelerates significantly to prevent the object force increasing toward infinity. After $t \approx 20s$, the velocity of ego vehicle matches the velocity of the object vehicle and maintains a safe braking distance between them. This scenario demonstrates an adaptive cruise control (ACC) function in the social-force based autonomous driving scheme. The flexibility of the proposed model excludes the need of specific rules defined for each traffic scenario.

The second scenario represents a 4-lane road where there is a slow vehicle in front (FIGURE 5). The major difference from the first scenario is the existence of empty lanes allowing the ego vehicle to change its lane. The initial conditions are shown in TABLE 2. As in the first scenario, the ego vehicle accelerates due to the initial target force then decelerate to compensate the increase in the object force as the ego vehicle approaches the object. In this case, the ego vehicle is affected by the object forces from the two vehicles in lane 3 and 4. As the NMPC tries to minimize the cost function in (15), the ego-vehicle is encouraged to perform a lane change from lane 3 to lane 2. A peak of lane force appears as the vehicle from the center of lane 3 to that of lane 2 in (5) and adjusts its heading angle in (7). An increase in target force is also observed as the vehicle slows down and steer away from lane 3. The combined amount of increase in the target and lane forces is still minimal compared to the potential increase in the object force when the lane-changing behavior is delayed or not executed. This is the benefit of the use of the NMPC formulation in (16), which evaluates the cost for the given prediction horizon.

TABLE 3. INITIAL CONDITION OF THE THIRD SCENARIO

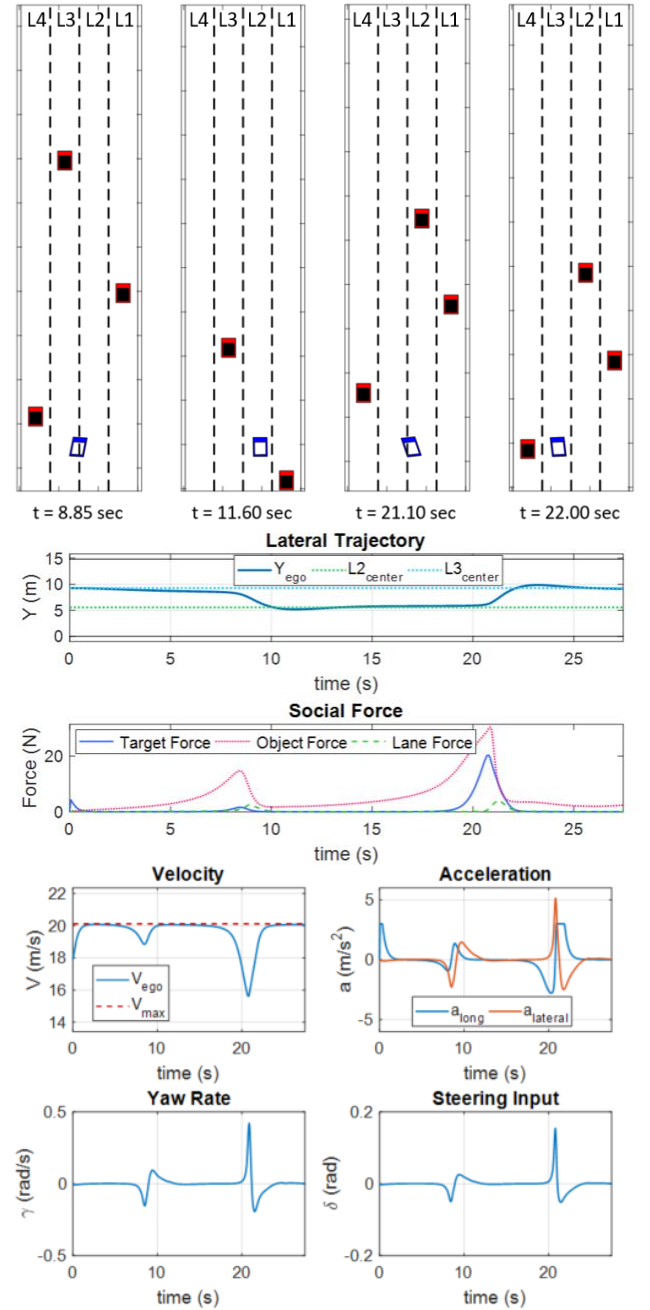| Vehicle	X (m)	Lane Number	V (m/s)
Ego	0	3	17.89
Object 1	150	4	3.58
Object 2	200	3	4.47
Object 3	170	1	4.47
Object 4	350	4	3.58
Object 5	380	2	4.02
Object 6	370	1	3.58

FIGURE 6. RESULTS OF THE THIRD SCENARIO (BLUE: EGO VEHICLE, RED: OBJECT VEHICLES)

The third scenario illustrates a case with the presence of additional object vehicles (FIGURE 6). The ego vehicle encounters a group of three object vehicles twice during the given similar amount of time as the second scenario. The initial condition of the third scenario is listed in TABLE 3. FIGURE 6 shows the ego vehicle changing its lane from lane 3 to lane 2 at $t \approx 8.85s$ as it sees a group of vehicles and especially an object vehicle (Object 2) traveling at 4.47 m/s in the lane 3. At $t \approx 21.10s$, the ego vehicle changes its lane once again due to the

slow vehicle (Object 5 in lane 2) in front. Object 5 is even slower (v = 4.02 m/s) than Object 2 (v = 4.47 m/s), and the ego vehicle is still experiencing the object forces from the first group of vehicles as they are still traveling toward the same direction. Therefore, the second lane-change is more delayed and more aggressive compared to the first lane-changing behavior.

CONCLUSION

In this paper, a human-like autonomous driver model is presented. The social aspect of human driving behavior is captured using a modified social force model (SFM) which is then implemented for predictive guidance and control via a nonlinear model predictive control (NMPC) framework.

The proposed driver model showed good performance and proper behavior in various simulated scenarios which include single-lane, as well as multi-lane traffic situations. The ego vehicle was able to prevent collision when there was a slow-traveling vehicle in front and perform adaptive cruise control (ACC) adjusting its speed to that of the slow vehicle, and it was also able to change its lane when there was an available option. Most importantly, the ego vehicle was able to perform such tasks while maintaining reasonable vehicle dynamic response.

In future work, the proposed model will be compared to a real traffic data to validate the similarity between the model and the real human driving behavior in various traffic scenarios. Once it is verified, this model will be used to study the behavior of autonomous vehicles employing this control scheme in a hybrid traffic where fully autonomous vehicles (AVs) and HOVs coexist. The line of work can have potential impact in how V2V and other connected automated vehicle technologies should be deployed in the mixed traffic environment.

APPENDIX

TABLE 4. BASIC VEHICLE DYNAMICS PARAMETERS

Parameter	Value
C_1	5000 (N/rad)
C_2	7000 (N/rad)
m	1870 (kg)
a	1.27 (m)
b	1.65 (m)
J_z	3000 (kg/m^2)

REFERENCES

[1]. Anderson, Jeffery R., Beshah Ayalew, and T. Weiskircher. "Modeling a professional driver in ultra-high performance maneuvers with a hybrid cost MPC." American Control Conference (ACC), 2016. IEEE, 2016.

[2]. El Hajjaji, A., and M. Ouladsine. "Modeling human vehicle driving by fuzzy logic for standardized ISO double lane change maneuver." Robot and Human Interactive Communication, 2001. Proceedings. 10th IEEE International Workshop on. IEEE, 2001.

[3]. Markkula, Gustav, et al. "A review of near-collision driver behavior models." Human factors 54.6 (2012): 1117-1143.

[4]. Bucchi, Alberto, Cesare Sangiorgi, and Valeria Vignali. "Traffic psychology and driver behavior." Procedia-Social and Behavioral Sciences 53 (2012): 972-979.

[5]. Gu, Yanlei, et al. "Human-like motion planning model for driving in signalized intersections." IATSS research 41.3 (2017): 129-139.

[6]. Yu, Hongtao, H. Eric Tseng, and Reza Langari. "A human-like game theory-based controller for automatic lane changing." Transportation Research Part C: Emerging Technologies 88 (2018): 140-158.

[7]. Helbing, Dirk, and Peter Molnar. "Social force model for pedestrian dynamics." Physical review E 51.5 (1995): 4282.

[8]. Li, Maosheng, Feng Shi, and Dafei Chen. "Analyze bicycle-car mixed flow by social force model for collision risk evaluation." 3rd International Conference on Road Safety and Simulation. 2011.

[9]. Qu, Zhao-wei, et al. "Modeling electric bike–car mixed flow via social force model." Advances in Mechanical Engineering 9.9 (2017): 1687814017719641.

[10]. Guo, L. Y., et al. "Modelling and simulation of vehicle behaviours based on the social force model." Information Science and Electronic Engineering: Proceedings of the 3rd International Conference of Electronic Engineering and Information Science (ICEEIS 2016), January 4-5, 2016, Harbin, China. CRC Press, 2016.

[11]. Weinan, Huang, and Fellendorf Martin. "Social Force Based Vehicle Model for Traffic Simulation." (2012).

[12]. Di Cairano, Stefano, et al. "Stochastic MPC with learning for driver-predictive vehicle control and its application to HEV energy management." IEEE Transactions on Control Systems Technology 22.3 (2014): 1018-1031.

[13]. Rowell, Stuart, Atanas A. Popov, and Jacob P. Meijaard. "Predictive control to modelling motorcycle rider steering." International journal of vehicle systems modelling and testing 5.2-3 (2010): 124-160.

[14]. Prokop, Günther. "Modeling human vehicle driving by model predictive online optimization." Vehicle System Dynamics 35.1 (2001): 19-53.

[15]. Wang, Qian, Thomas Weiskircher, and Beshah Ayalew. "Hierarchical hybrid predictive control of an autonomous road vehicle." ASME 2015 Dynamic Systems and Control Conference. American Society of Mechanical Engineers, 2015.

[16]. Wang, Qian, and Beshah Ayalew. "Constraint tightening for the probabilistic collision avoidance of multi-vehicle groups in uncertain traffic." Control Technology and Applications (CCTA), 2017 IEEE Conference on. IEEE, 2017.

[17]. Kurt, Arda, and Ümit Özgüner. "Hierarchical finite state machines for autonomous mobile systems." Control Engineering Practice 21.2 (2013): 184-194.

[18]. Wang, Qian, Beshah Ayalew, and Thomas Weiskircher. "Optimal assigner decisions in a hybrid predictive control of

an autonomous vehicle in public traffic." American Control Conference (ACC), 2016. IEEE, 2016.

[19].Y. Koren and J. Borenstein, "Potential field methods and their inherent limitations for mobile robot navigation," Proceedings. 1991 IEEE International Conference on Robotics and Automation, Sacramento, CA, 1991, pp. 1398-1404 vol.2.

[20].Shimoda, Shingo, Yoji Kuroda, and Karl Iagnemma. "Potential field navigation of high speed unmanned ground vehicles on uneven terrain." Robotics and Automation, 2005. ICRA 2005. Proceedings of the 2005 IEEE International Conference on. IEEE, 2005.

[21].Genta, Giancarlo. Motor vehicle dynamics: modeling and simulation. Vol. 43. World Scientific, 1997.

[22].Grne, Lars, and Jrgen Pannek. "Nonlinear model predictive control: theory and algorithms." (2013).

[23].Wang, Qian, and Beshah Ayalew. "A multiple vehicle group modelling and computation framework for guidance of an autonomous road vehicle." American Control Conference (ACC), 2017. IEEE, 2017.